Int J Adv Manuf Technol (2005) 25: 343–349
DOI 10.1007/s00170-003-1921-6

ORIGINAL ARTICLE

Tao Chen · Peiqing Ye · Jinsong Wang

Local interference detection and avoidance in five-axis NC machining of sculptured surfaces

Received: 11 May 2003 / Accepted: 18 August 2003 / Published online: 3 November 2004

Abstract The tool interference problem is the most critical problem faced in sculptured surface machining. This paper presents a methodology for interference detection and avoidance in five-axis NC machining of sculptured surfaces with a filleted-end cutter. The surfaces to be machined are divided into convex and non-convex regions. There is no local interference inside the convex regions. For the non-convex regions, based on the analysis of the different local interference, local gouging is first detected and avoided by determining optimal cutter orientations. Rear gouging detection and avoidance algorithms are then proposed for simple smooth surfaces and complex shaped surfaces, respectively. The techniques presented in this paper can be used to generate interference-free tool paths. The realistic results indicate that the proposed method is feasible and reliable.

Keywords Filleted-end cutter · Five-axis NC machining · Local gouging · Rear gouging · Sculptured surfaces

1 Introduction

Five-axis numerically controlled (NC) machining of sculptured surfaces has been widely applied in the aerospace, shipbuilding, automotive, glassware, ceramics, and dies and moulds industries. Because of the two additional degrees of freedom, five-axis NC machining offers some advantages over 3-axis machining. However, five-axis machining suffers from some problems such as a large investment, and complex algorithms for tool interference detection and avoidance, etc. The tool interference problem is the most critical problem faced in sculptured surface machining.

T. Chen (✉) · P. Ye · J. Wang
Manufacturing Engineering Institute,
Department of Precision Instruments,
Tsinghua University,
Beijing, P.R. China
E-mail: chentao02@tsinghua.org.cn

Tool interference in five-axis NC machining of sculptured surfaces can be classified into two types: (1) global interference – the tool flank surface collides with the machined surfaces and fixtures in the machining environment and (2) local interference. In this paper, the focus is on local interference. Local interference includes local gouging and rear gouging [1, 2] as shown in Fig. 1. Portions of the cutter's leading edge sometimes extend below the designed surface, removing more material than is allowed by the designed surface profile tolerance. This leads to local gouging (Fig. 1a). Local gouging occurs when the radius of the local surface curvature is smaller than that of the cutter. Rear gouging is a similar effect caused by the trailing edge or the cutting bottom of the cutter (Fig. 1b,c). Rear gouging may be caused by using a large size cutter or by choosing an improper cutter orientation.

The detection and avoidance of tool interference is a tough problem. Many researchers have studied the interference problem, but most concentrate on interference detection and avoidance in three-axis NC machining. In five-axis NC machining of sculptured surfaces, the tool interference problem is much more acute because of the complex tool movements and the irregular curvature distributions of sculptured surfaces. Jensen et al. [3] inclined a flat-end cutter to the normal at the cutter contact (CC) point on a sculptured surface based on matching the curvature of the instantaneous cutting profile of the cutter to that of the sculptured surface at the CC point, to eliminate local gouging. Choi et al. [4] proposed a method for generating optimal cutter location (CL) points from CC points by formulating a constrained minimization problem based on the instantaneous cutting profile of the cutter. Li et al. [5] presented an efficient algorithm for generating interference-free tool paths for sculptured surfaces. Lee et al. [6–8] have developed algorithms to eliminate collisions and rear gouging. They also address issues of local gouging prevention [9]. Sarma [1] presented a new method to detect and eliminate rear gouging in the five-axis NC machining of sculptured surfaces with flat-end cutters. The method is based on finding accurately the instantaneous cutting profile of the cutter that enables rear gouging detection and elimination calculations to be done in two dimensions. Rao et al. [10] compared the normal

Fig. 1. Local interference

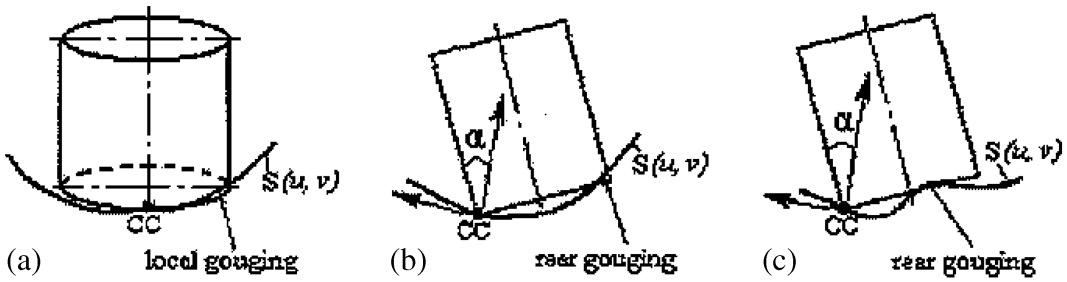

curvatures of the machined surface and the cutter swept surface, in all directions in the tangent plane of the machined surface at the CC point. Based on this comprehensive curvature matching, local gouging in the five-axis machining of sculptured surfaces using flat-and cutters is detected and eliminated. Very little work has been done on tool interference detection and avoidance of the filleted-end cutter. Lee et al.'s work [8] is one example.

In this paper, we present a systematic methodology for investigating the tool interference in five-axis NC machining of sculptured surfaces using filleted-end cutters. The surfaces to be machined are divided into convex and non-convex regions. There is no local interference inside the convex regions. For the non-convex regions, the tool interference is solved in three phases according to three scenarios. In phase I, an optimal cutter orientation is first determined by matching the instantaneous cutting profile of the cutter and the machined surface, as close as possible to avoid local gouging. In phase II, rear gouging detection and avoidance is implemented by calculating the intersection between the offset surface of the machined surface and the offset cylinder of the cutter, for simple smooth surfaces. In phase III, for cases of complex shaped surfaces, a search for possible rear gouging is conducted by first dividing the machined surfaces into a set of triangular facets. Rear gouging is then detected by classifying the relative position of the bottom plane of the cutter and the vertices of the triangular facets. If one of the vertices of the triangles under the cutter shadow is above the bottom plane of the cutter, rear gouging will occur. If any rear gouging is detected, the cutter orientation is adjusted to eliminate gouging. The process continues until all the CC data are checked.

2 Cutter description and cutter orientation

There are many types of cutters used in milling applications. An end-mill cutter is often the choice for sculptured surface machining. Basically three types of end-mill cutters are used in the 5-axis NC machining of sculptured surfaces: the flat-end cutter, the fillet-end cutter and the ball-end cutter. A model of a fillet-end cutter can easily represent both the flat-end cutter and the ball-end cutter. For this reason, this paper will consider 5-axis sculptured surface machining with a fillet-end cutter, and with the flat-end cutter and the ball-end cutter as special cases.

A filleted-end cutter consists of a plane that serves as the bottom surface, and a piece of a torus connected to a cylinder, as shown in Fig. 2. The cutting surface $T(\phi, \theta)$ of a filleted-end

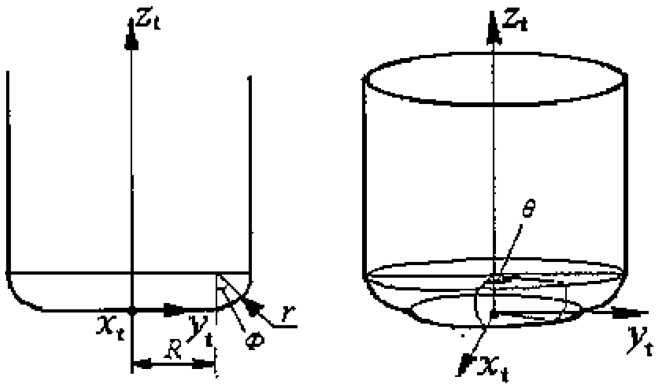

Fig. 2. Filleted-end cutter

cutter can be represented by a two parameter surface with continuous derivatives as in Eq. 1:

$$T(\phi, \theta) = \begin{bmatrix} (R + r\sin\phi)\cos\theta \\ (R + r\sin\phi)\sin\theta \\ r(1 - \cos\phi) \\ 1 \end{bmatrix} \tag{1}$$

where R is the radius of the bottom portion, r is the fillet radius of the cutter, ϕ describes the corner portion and $\phi \in [0, \pi/2]$, and θ is the angle from the X_t-axis and $\theta \in [0, 2\pi]$.

In 5-axis machining, besides the translations along the three translation axes of an NC machine, the cutter can be rotated about two of the three translation axes. As shown in Fig. 3, the

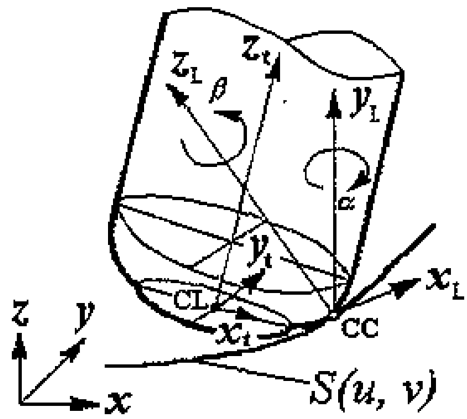

Fig. 3. Cutter orientation

local coordinate system $(X_L - Y_L - Z_L)$ is set up at the CC point. The X_L-axis is along the tangent of the tool path in the instantaneous cutting direction and the Z_L-axis is along the normal of the surface at the CC point. The Y_L-axis is defined by the X_L-axis and Z_L-axis, using the right-hand rule. First, the cutter is rotated around the Y_L-axis, while the CC point is the pivot. The first rotation angle is defined as the inclination angle α. Secondly, the cutter is rotated around the Z_L-axis, while the CC point is the pivot. The second rotation angle is defined as the tilt angle β. These two angles completely define the orientation of the cutter [2].

Marciniak [11] concluded that the largest machined strip width (or the largest material removal) is obtained when the CC point moves along a curve of the smaller principle curvature, and the tool position is at the tilt angle $\beta = 0$. Thus, we choose the X_L-axis as the direction of tool motion and rotate the cutter by an inclination angle α about the Y_L-axis. This is accomplished by pre-multiplying by the following rotation matrix R_y:

$$R_y = \begin{bmatrix} \cos\alpha & 0 & -\sin\alpha & 0 \\ 0 & 1 & 0 & 0 \\ \sin\alpha & 0 & \cos\alpha & 0 \\ 0 & 0 & 0 & 1 \end{bmatrix}$$

which gives an equation for the cutter rotated about the Y_L-axis as shown in Eq. 2:

$$\begin{aligned} E(\phi,\theta) &= R_y \bullet T(\phi,\theta) \\ &= \begin{bmatrix} \cos\alpha\,(R + r\sin\phi)\cos\theta - r\,(1-\cos\phi)\sin\alpha \\ (R + r\sin\phi)\sin\theta \\ \sin\alpha\,(R + r\sin\phi)\cos\theta + r\,(1-\cos\phi)\cos\alpha \\ 1 \end{bmatrix} \end{aligned} \tag{2}$$

3 Surface interrogation by differential geometry

3.1 Surface properties

For a sculptured surface $S(u, v)$, which is its unit normal vector at point (u, v) can be calculated:

$$\mathbf{n}(u, v) = \frac{\mathbf{S}_u \times \mathbf{S}_v}{|\mathbf{S}_u \times \mathbf{S}_v|}\,, \tag{3}$$

where $\mathbf{S}_u$ and $\mathbf{S}_v$ are the tangent vectors along u- and v-parametric directions.

The surface properties are characterized by the first and second fundamental forms of differential geometry. The first fundamental form provides us metrical properties of surfaces such as measurement of lengths, areas and angles between two curves on the surface. The second fundamental form allows us to analyze the surface curvature at a given point. Using the first and second fundamental forms, several important geometric properties can be described. The important geometric properties of a surface are the Gaussian curvature K and the mean curvature H:

$$\begin{aligned} K &= \frac{LN - M^2}{EG - F^2}, \\ H &= \frac{2FM - EN - GL}{2\left(EG - F^2\right)}\,, \end{aligned} \tag{4}$$

where E, F, G and L, M, N are the magnitudes of the first and second fundamental forms, respectively:

$$E = \mathbf{S}_u \cdot \mathbf{S}_u, \quad F = \mathbf{S}_u \cdot \mathbf{S}_v, \quad G = \mathbf{S}_v \cdot \mathbf{S}_v \tag{5}$$

$$L = \mathbf{n} \cdot \mathbf{S}_{uu}, \quad M = \mathbf{n} \cdot \mathbf{S}_{uv}, \quad N = \mathbf{n} \cdot \mathbf{S}_{vv}\,. \tag{6}$$

The Gaussian curvature describes the local shape of a surface. The mean curvature measures the deviation of a surface from the minimal surface: these are surface with mean curvature equal to zero everywhere.

The principal curvatures are the upper and lower bounds of the normal curvature at a given point and their corresponding direction are called principal directions of curvature and are generally orthogonal except at umbilical points. The principal curvatures are given by:

$$\begin{aligned} \kappa_{\max} &= H + \sqrt{H^2 - K}, \\ \kappa_{\min} &= H - \sqrt{H^2 - K}\,. \end{aligned} \tag{7}$$

3.2 Surface shape classification

To avoid tool interference in machining, it is important to analyze the local surface shape. The purpose of local surface shape classification is to identify the convex and non-convex regions, which provide the efficient candidates for detecting and avoiding the tool interference.

To classify the surface, a value K' is defined as:

$$K' = LN - M^2\,.$$

Based on the values of K', K and H, the surface points can be divided into four different types, as shown in the following [12]:

1. Convex elliptic point: If $K' > 0$ and $H < 0$, the surface lies entirely on the surface normal side (n) of the tangent plane in its neighborhood. Both the principal curvatures are negative (i.e., $K > 0$ and $H < 0$).
2. Concave elliptic point: If $K' > 0$ and $H > 0$, the surface lies entirely on the opposite side (-n) of the tangent plane in its neighborhood. Both the principal curvatures are positive (i.e., $K > 0$ and $H > 0$).
3. Hyperbolic point (Saddle point): If $K' < 0$, the surface lies entirely on both sides of the tangent plane in its neighborhood. Both the principal curvatures have different signs (i.e., $K < 0$).
4. Parabolic point: If $K' = 0$, the surface is a parabolic point. There is at least a single line in the tangent plane along which the curvature is zero (i.e., $K = 0$).

The region composed of convex elliptic points is defined as a convex region, and the other region is called a non-convex region. In interference detection, the surface points are sampled first, and the E, F, G, L, M, N values are calculated at these points, respectively. With the K' and H values, the convex and non- convex regions can be identified. Different kinds of shapes on a surface can be treated with the different interference detection algorithm. If the surface is locally convex, an end-mill cutter may be oriented and positioned such that the cutter axis points in the positive direction of the surface normal, at the cutter contact point, so the local interference is automatically avoided. If the surface is locally non-convex, local interference may arise. Interference detection and avoidance will thus be necessary in non-convex regions, which will be discussed in the following sections.

4 Interference detection and avoidance algorithm

As stated above, for the non-convex regions, local interference may arise. It is necessary to detect and avoid this local interference in non-convex regions. In this section, the local interference is solved in three phases according to the three scenarios as shown in Fig. 1.

4.1 Phase I: local gouging detection and avoidance

First, local gouging as shown in Fig. 1a is discussed as follows.

The effective cutting curvature of the filleted-end cutter in the plane orthogonal to tool motion can be calculated in terms of the curvature formula [13] by using Eq. 2 as follows:

$$\kappa_{eff} = \frac{\left|\dot{y}(\theta)\,\ddot{z}(\theta) - \ddot{y}(\theta)\,\dot{z}(\theta)\right|}{\left[\dot{y}^2(\theta) + \dot{z}^2(\theta)\right]^{3/2}} ,$$

where

$$y(\theta) = (R + r\sin\phi)\sin\theta$$
$$z(\theta) = \sin\alpha\,(R + r\sin\phi)\cos\theta + r\,(1 - \cos\phi)\cos\alpha .$$

Since the angle θ is equivalent to zero at the CC point, the effective cutting curvature of the filleted-end cutter in the plane orthogonal to tool motion can be given:

$$\kappa_{\text{eff}} = \frac{\sin\alpha}{R + r\sin\alpha} . \tag{8}$$

As illustrated in Fig. 1a, local gouging occurs if and only if the machined surface maximum principal curvature is greater than the effective cutting curvature of the cutter [10]. To avoid local gouging, the following condition must be satisfied:

$$\kappa_{\max} \le \kappa_{\text{eff}} , \tag{9}$$

where $\kappa_{\max}$ is the maximum principal curvature of the machined surface which can be calculated by Eq. 7.

Using this condition the smallest value of the inclination angle α, that would avoid local gouging and ensure the largest machining strip (or the largest material removal), may be calculated as follows:

$$\alpha = \sin^{-1}\left(\frac{R\kappa_{\max}}{1 - r\kappa_{\max}}\right) . \tag{10}$$

When the inclination angle is smaller than the value of α estimated using Eq. 10, it may easily cause local gouging. A much larger inclination angle may extend the tool path length as well as the NC machining time, which causes low machining efficiency. Therefore, to improve the machining productivity and to avoid gouging in five-axis machining, it is desired to match as close as possible the instantaneous cutting profile of the cutter and the machined surface.

4.2 Phase II: rear gouging detection and avoidance for simple smooth surfaces

In phase I, the cutter inclination angle α is adjusted according to the local surface shape to avoid local gouging. A small α can also cause rear gouging when machining a concave surface as illustrated in Fig. 1b. In phase II, as shown in Fig. 4, the filleted-end cutter is offset inwards by the cutter-corner radius r, and the line segment is offset to be a cylinder with axis Z_C and radius R. We then calculate the intersection between this full cylinder and the offset surface $\tilde{S}(u, v)$ to detect rear gouging.

As shown in Fig. 4, the local coordinate system ($X_C - Y_C - Z_C$) is defined at the center point **0**. The X_C-axis is defined along the cutting direction, and Z_C-axis is defined along the tool axis. The Y_C-axis is defined with respect to the X_C-axis and Z_C-axis, using the right-hand rule. The analytical function of the cylinder, with axis Z_C and radius R, is as follows:

$$x_c^2 + y_c^2 \le R^2 , \quad z_c \text{ can be any value} .$$

Let $S(u, v)$ be a parametric surface. Then, an offset surface $\tilde{S}(u, v)$ with an offset distance r (the fillet radius of the cutter) is

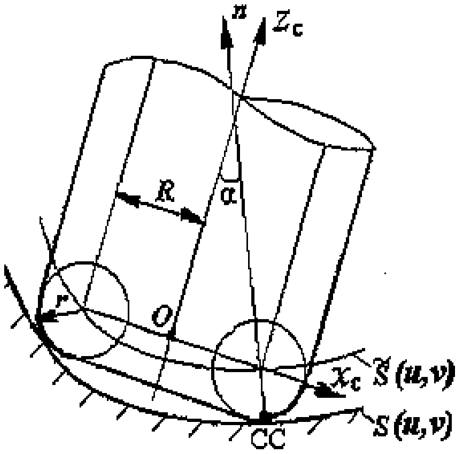

Fig. 4. Rear gouging detection

computed by:

$$\tilde{S}(u, v) = S(u, v) + r\mathbf{n}, (u, v)$$

where $n(u, v)$ is the normal vector to the surface $S(u, v)$ at point (u, v) and it can be calculated by the Eq. 3.

Rear gouging may occur if one of the points of intersection between the full cylinder and the offset surface $\tilde{S}(u, v)$ has a positive Z_C-coordinate in the local coordinate system $(X_C - Y_C - Z_C)$. If so, rear gouging can be avoided by inclining the cutter (or increasing the inclination angle α) more.

4.3 Phase III: rear gouging detection and avoidance for complex surfaces

The solution for rear gouging detection and avoidance is complicated for 5-axis machining. For simple smooth surfaces, the above method works well for rear gouging avoidance. For cases of a large cutter or a complex shaped (high-curvature) surface, the gouging control in Phase II may not be sufficient for preventing potential rear gouging as illustrated in Fig. 1c. In phase III, the machined surface is first divided into a set of triangular facets. Rear gouging is then detected by classifying the relative position of the bottom plane of the cutter and the vertices of the triangular facets. If one of the vertices of the triangles under the cutter shadow is above the bottom plane of the cutter, rear gouging will occur. In this case, a larger inclination angle α is required to avoid rear gouging.

4.3.1 Surface triangulation

The procedure for 5-axis interference detecting and avoiding is very time-consuming, and it is difficult to complete on parametric surfaces. The algorithm for tessellating a surface into a set of triangulations within a certain tolerance is investigated here. Interference checking between the cutter and the surface can thus be converted into the checking of interference between the cutter and those triangles.

A simple method for surface triangulation is to take discrete points with constant u/v intervals from iso-parametric curves. Thus a polyhedral model of the surface that consists of those surface points can be obtained. As shown in Fig. 5, the procedure of surface triangulation can be stated as follows:

1. The surface is first divided into a series of quadrangles in parametric space. Each quadrangle is then split into two triangles by joining the diagonals of the quadrangle (Fig. 5a).
2. Mapping triangles from parametric space into Cartesian space (Fig. 5b).
3. Checking the deviation of each of the triangles as discussed in Eq. 12.
4. If the largest value of these two deviations is greater than the specified tolerance, then the quadrangle is divided into four smaller quadrangles and each quadrangle broken into two triangles.
5. The two triangles for each of the smaller rectangles are then checked for deviations until all triangles meet the deviation requirements.

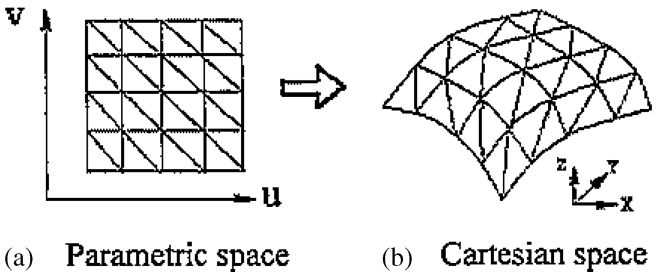

Fig. 5a,b. Surface triangulation **a** Parametric space **b** Cartesian space

To evaluate the quality of the surface triangulation, suppose it is desired to triangulate a parametric surface $\mathbf{S}(u, v)$. One of the approximating triangles would be as shown in Fig. 6. The vertices of the triangle will be $\mathbf{S}_1(u_1, v_1)$, $\mathbf{S}_2(u_2, v_2)$ and $\mathbf{S}_3(u_3, v_3)$. The triangle is formed by linearly blending the lines S_1S_2 and S_1S_3. Therefore, any point on the triangle is given by:

$$T(s, t) = (1 - s)\, S_1 + (s - st)\, S_2 + (ts)\, S_3 .$$

The corresponding point on the triangular surface patch will be given by the parameters:

$$\begin{aligned} u &= (1 - s)\, u_1 + (s - st)\, u_2 + (st)\, u_3 , \\ v &= (1 - s)\, v_1 + (s - st)\, v_2 + (st)\, v_3 , \end{aligned} \tag{11}$$

where $0 \le s, t \le 1$.

To tell if the triangulation accurately reflect the topology of the surface, a measure of the "goodness" of the triangulation of the surface is needed. A good measure would be to measure the maximum point distance between the surface and the triangle at specific positions [Fig. 6]. The deviation can then be formulated as:

$$\max(\text{deviation}) = \max\{\text{dist}(S(u(s, t), v(s, t)), T(s, t))\} . \tag{12}$$

This function calculates the distance between the triangle and the surface at particular (s, t) pairs and the corresponding (u, v) pair given by Eq. 11 and takes the maximum value.

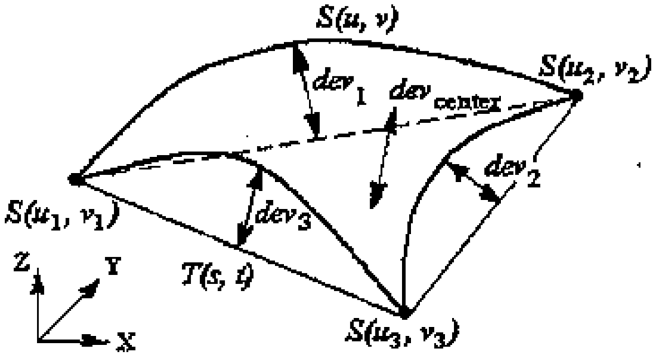

Fig. 6. Approximate deviation checking

4.3.2 Rear gouging detecting and avoidance algorithm

After triangulation, each triangle can be described by a list data structure, including:

- Three vertices in counterclockwise order
- Topological relations among triangles
- A flag to locate which triangle has been checked

All triangles to be checked are put onto a stack. To simplify rear gouging detection, we transform both the cutter and the triangles to a space in which the cutter axis is parallel to the $+z$ axis. After the transformation, the projection of the cutter onto the xy plane is a disc. Triangles whose xy projections overlap the disc are checked for rear gouging. Given a triangle, rear gouging may happen only when at least one of its vertices is above the bottom plane of the cutter.

Let $\boldsymbol{T}$ be the unit normal of the bottom plane of the cutter and $\boldsymbol{Q}_0$ be a point (it can be the center) on the plane. Let $\boldsymbol{P}$ is a vertex on a triangle. We may express the bottom plane of the cutter as:

$$(\boldsymbol{Q} - \boldsymbol{Q}_0) \cdot \boldsymbol{T} = 0 \,.$$

The distance between point $\boldsymbol{P}$ and the bottom plane of the cutter is equal to: $(\boldsymbol{P} - \boldsymbol{Q}_0) \cdot \boldsymbol{T}$.

If $(\boldsymbol{P} - \boldsymbol{Q}_0) \cdot \boldsymbol{T} > 0$: the vertex is above the bottom plane of the cutter. The triangular facet will interfere with the cutter.

If $(\boldsymbol{P} - \boldsymbol{Q}_0) \cdot \boldsymbol{T} = 0$: the vertex is on the bottom plane of the cutter. The triangular facet may be interference-free.

If $(\boldsymbol{P} - \boldsymbol{Q}_0) \cdot \boldsymbol{T} < 0$: the vertex is below the bottom plane of the cutter. The triangular facet will be interference-free.

The rear gouging detection begins with the triangle on which the CC point lies. If there is no gouging at this starting triangle, its three neighbors are the next candidates for rear gouging checking. Once the rear gouging is found, the cutter orientation will be adjusted and the interference detection procedure will be repeated from the starting triangle where the CC point sits. The detection loop continues until either the stack is empty or the loop is infinite. An infinite loop happens if the loop number is larger than the pre-selected maximum loop number. In the case of an infinite loop, the rear gouging detection fails.

5 Examples

The method presented in this paper has been successfully implemented in the visual C++ programming language using the ACIS geometric modeler on the personal computer (PC), Intel Pentium IV processor at 2.0 GHz under the Windows XP operating system. Figure 7 shows the examples of interference-free tool paths generated using the proposed method.

6 Conclusions

This paper presents a systematic methodology for investigating the tool interference in the five-axis NC machining of sculptured surfaces using filleted-end cutters. The surfaces to be machined are divided into convex and non-convex regions. There is no local interference inside the convex regions. For non-convex regions, the method includes determining the optimal cutter orientation to avoid local gouging and updating the inclination angle to prevent rear gouging. In the first phase, an optimal cutter orientation is first determined by matching the instantaneous cutting profile of the cutter and the machined surface as close as

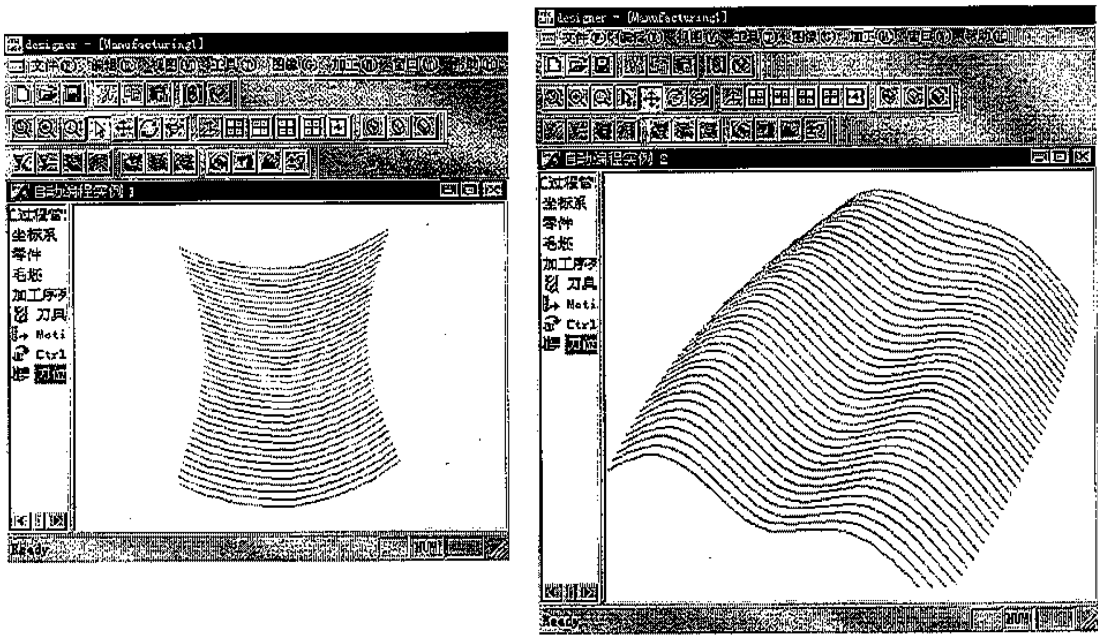

Fig. 7. Interference-free tool path

possible to avoid local gouging. In the second phase, rear gouging detection and avoidance is implemented by calculating the intersection between the offset surface of the machined surface and the offset cylinder of the cutter, for simple smooth surfaces. In the third phase, for cases of complex shaped surfaces, a search for possible rear gouging is conducted by first dividing the machined surfaces into a set of triangular facets. Rear gouging is then detected by classifying the relative position of the bottom plane of the cutter and the vertices of the triangular facets. If one of the vertices of the triangles under the cutter shadow is above the bottom plane of the cutter, rear gouging will occur. If any rear gouging is detected, the cutter orientation is adjusted to eliminate gouging. The process continues until all the CC data are checked. The methodology presented in this paper can be used to support automatic programming of five-axis NC machining. Realistic results indicate that the proposed method is feasible and reliable.

In addition, the model of the filleted-end cutter can easily be used to represent both a flat-end cutter (by choosing a radius $r = 0$) and a ball-end cutter (by choosing a radius $R = 0$). Therefore, the algorithm proposed in this paper may be suited for both flat-end cutters and the ball-end cutters.

Acknowledgement This work was supported by the National 863 Program of China under grant number 863-402- 2001AA423260. Their support is greatly appreciated. The authors are grateful to the anonymous reviewers of this paper for their valuable remarks.

References

1. Sarma R (1998) Rear gouge detection and elimination in five-axis NC machining of sculptured surfaces, Trans of the NAMRI/SME, 26, pp 225–230, 1998
2. Lo CC (1999) Efficient cutter-path planning for five-axis surface machining with a flat-end cutter. Comput Aided Des 31:557–566
3. Jensen CG, Anderson DC (1993) Accurate tool placement and orientation for finish surface machining. J Des Manuf 3(4):251–261
4. Choi BK, Park JW, Jun CS (1993) Cutter-location data optimization in 5-axis surface machining. Comput Aided Des 25(6):377–386
5. Li SX, Jerard RB (1994) 5-axis Machining of Sculptured Surfaces with Flat-end Cutter. Comput Aided Des 26(3):165–178
6. Lee YS, Chang TC (1995) 2-phase approach to global tool interference avoidance in 5-axis machining. Comput Aided Des 27(9):715–729
7. Lee YS (1997) Filleted endmill placement problems and error analysis for multi-axis CNC machining. Trans of the NAMRI/SME 25, pp 129–134
8. Lee YS (1997) Admissible tool orientation control of gouging avoidance for 5-axis complex surface machining. Comput Aided Des 29(7):507–521
9. Lee YS, Ji H (1997) Surface interrogation and machining strip evaluation for 5-axis CNC die and mold machining. Int J Prod Res 35(1): 225–252
10. Rao A, Sarma R (2000) On local gouging in five-axis sculptured surface machining using flat-end tools. Comput Aided Des 32:409–420
11. Marciniak K (1987) Influence of surface shape on admissible tool positions in 5-axis face milling. Comput Aided Des 19(5):233– 236
12. Hosaka M (1992) Modeling of curves and surfaces in CAD/CAM. Springer, Berlin Heidelberg New York
13. Wu DR (1982) Lectures on differential geometry. The People's Education Press, Beijing